Kite Foil Mast Ventilation Study

MARINE 2021

S. Bartesaghi[1,*], G. Provinciali[2] and F. Lovato[3]

[1] Milano, Italy. E-mail: simone.bartesaghi@gmail.com, fluid4engineering@gmail.com, web page: http://www.fluid4engineering.com

[2] Lecco, Italy. E-mail: g.provinciali@gmail.com

[3] Monza, Italy. E-mail: franco.lovato90@gmail.com
[*] Corresponding author: S. Bartesaghi, simone.bartesaghi@gmail.com

ABSTRACT

Considering the evolution of the racing sailing yacht in the last decade, we have seen the increasingly extensive use of hydrofoil systems able to support and fly boats over the free surface. The great advantage of these systems is to increase comfort in navigation and to reduce drag. Unfortunately, these systems, in addition to the great advantages in terms of efficiency, bring with them problems linked above all to their functioning between two fluids, air and water.
In fact, the hydrofoils systems are subjected to natural ventilation and cavitation. In particular, the phenomenon of ventilation is typically present when there is a surface piercing strut that includes air and water in particular conditions of use; the geometry and physical conditions allow the creation of a region with a lower pressure than the atmospheric one, which then causes a cavity connected to the external environment. Ventilation is therefore an important phenomenon to be taken into consideration when designing hydrofoil appendages for racing boats and understanding the phenomena is fundamental for the success of the project.
Using the numerical simulation, in this case CFD, it is possible to investigate the favorable conditions of formation of the ventilated cavity for the conditions of use of a foil appendage. In order to use CFD as a forecasting and design tool, it was necessary to carry out a validation campaign using a reference benchmark; the results of the investigation made it possible to fine-tune the CFD tool to be able to predict the phenomenon of ventilation in a robust manner.
By applying the method developed on a kite foil surface piercing strut case, it was possible to estimate the performance differences of 2D sections and planform shapes to understand the ventilation tolerance of new candidate designs for construction. Furthermore, it was possible to visualize the ventilation trend by means of numerical indices able to visually show the behavior of one design compared to another. These methods could be used together with low fidelity methods (VLM, panel code, lifting line) to build response surfaces or surrogate models to be used in performances prediction..

Keywords: CFD, Hydrofoils, Ventilation, Optimization.

NOMENCLATURE

$AoA, AoAs$	Angle of attack, Angles of attack [deg]
AR_h	Submerged aspect ratio [-]
c	Section chord [m]
Cl	Hydrodynamic force coefficient (lift) in the y-direction [-]
Cd	Hydrodynamic force coefficient (drag) in the x-direction [-]
Cp	Pressure coefficient [-]
Fn_h	Depth based Froude number [-]
h	Strut Depth [m]
z	Distance from freesurface [m]
P	Hydrostatic pressure [Pa]
$Patm$	Atmospheric pressure [Pa]
U	Free stream velocity [m s^{-1}]
ΔT	Time step [s]
$\delta_{RE_{k1}}$	Estimated error [-]
$\epsilon_{k_{ij}}$	Grid solution numerical difference [-]
Fs	Safety factor [-]
p	Convergence order [-]
r_{ij}	Refinement ration [-]
R_k	Ratio of convergence [-]
U_k	Uncertainty [-]
α_b	Bifurcation angle [deg]
ρ	Fluid density [kg m^{-3}]
σ_c	Section cavitation number [-]
σ_v	Probability of ventilation inception [-]
d	Mahalanobis distance [-]
$\sum$	Covariance [-]
$\mathbf{y}$	Vector of the observations [-]
μ	Mean of observations [-]
CFD	Computational Fluid Dynamics
EFD	Experimental Fluid Dynamics
VLM	Vortex-Lattice Method

1 INTRODUCTION

Hydrofoil systems are not recent in the marine history. In fact lifting systems were introduced in the past for passenger and military boats. In the last decade they have been used extensively also on sailing boat, starting from the 34th Americas Cup (AC72 Class), evolved in the 35th Americas Cup (AC50 Class) and brought to the pinnacle of technology in the 36th Americas Cup (AC75 Class).

Since hydrofoil systems have proved to be flying steadily even at high speeds, many ideas and prototypes have been developed. For example, they have been used and tested on kite boards, the so called kite hydrofoil, which will become a discipline at the Paris Olympics in 2024.

As far as kite hydrofoil is concerned, it is a variant of the basic kite board with a lifting device connected to the board. The rider on his/her board is lifted out of the water so that the resistance is decreased and he/she rides at high speed even in light wind conditions. The kite hydrofoil system consists in a vertical strut (which acts as a surface piercing body) with two wings at the bottom (main and stabilizer).

The length of the strut allows the athlete to ride low or high above the water and must have the least resistance possible and a proper lifting capability. Due to the high-speed targets and the section design, the strut could be subject to cavitation and ventilation. The latter must be taken into account in the design of the strut surface since it brings about loss of lift and stability. The air inflated from the free surface trough the trailing edge of the strut changes suddenly the balance and the athlete can fall back in water and consequently lose the race.

The existing experimental tests are mostly based on riders reports, but Americas Cup derived technologies can now be exploited to develop and investigate new designs which consider free surface interaction, dynamic conditions and tests in virtual environments. Ventilation is the key factor for lifting devices as it determines performances and controllability (Taylor 1950; Breslin et al. 1959; Fridsma 1963; Swales et al. 1974). This phenomenon is given by local pressure near the body, when there is a lower pressure region with separated flow and a no-stop connection with air. Strut are subjected to natural ventilation due to the bodys penetration in the free surface that gives a space for air inflation.

Fully wetted, base-cavitating, partially cavitating and fully ventilated/supercavitating flow are four kind of regimes that can exists (Young *et al.* 2017; Young *et al.* 2013.). The first one occurs at small angle of attack where both sides of the strut are fully wetted. The second one is predominant when the maximum suction pressure reaches the cavity pressure causing the air to enter in the low-pressure system. The third one is when the cavity occurs only in a specific area and flows attaches again along the chord. Finally, the last one is established at large angle of attacks (AoAs ¿ 21°), where the suction pressure decreases and the cavity covers both the strut chord and span. Since this regime occurred in A-Class daggerboard with small AoAs, the attention was given to free surface perturbation; in fact, free surface perturbation can trigger ventilation, contrary to what the theory and data said on simple surfaces.

Flow scales with the depth-based Froude number (Fn_h) and the yaw angle as seen in Harwood *et al.* 2016, where Fn_h his a vital parameter to define possible ventilation regime. Yaw angle defines also the behavior of the ventilation (stable or unstable) with a limit, called bifurcation angle α_b, below that the regime is fully wetted. In case of fully ventilated flow, the regime is stable if Lift coefficient is:

$$Cl \geqslant 5Fn_h^{-2} \; with \; Fn_h \geqslant 3, \tag{1}$$

Section cavitation number (σ_c) also generates ventilated cavities; for natural ventilation, the cavity is open to the atmosphere and σ_c increases linearly with depth for a given Fn_h because of the hydrostatic pressure gradient. Considering a surface piercing strut with depth h:

$$\sigma_c(z) = \frac{z}{h} \cdot \frac{2}{Fn_h^2}, \tag{2}$$

Probability of ventilation inception (σ_v)is similar to σ_c and puts in relations the local pressure differential with the kinetic energy of the flow (Barden *et al.* ,2012):

$$\sigma_v = \frac{P - P_{atm}}{0.5\rho U^2}, \tag{3}$$

If this parameter has negative values, it indicates the possibility of ventilation inception. Here the depiction of a typical surface piercing strut. Tail ventilation or Taylor instability is a base-cavitation in blunt trailing edge devices, in which a cavity may develop aft of the feature. Studies on the AC50 daggerboards ventilation show a peculiar vortex structure able to predict the start of the ventilation, Binns (2017).

2 APPLICATION ON KITE FOIL STRUT

Typical conditions for upwind/downwind course in racing mode are 20 knots speed with high heel angle up to 60° for upwind and 40 knots speed with low heel angle for downwind. Generally, ventilation occurs in upwind condition despite the lower speed because of the higher heel angle, which means a working condition closer to the perturbed free surface and possibility of nose/tail ventilation. Picture shows the typical upwind condition where ventilation could be present; heel is rotation around x-axis, rake is rotation around y-axis and yaw is rotation around z-axis.

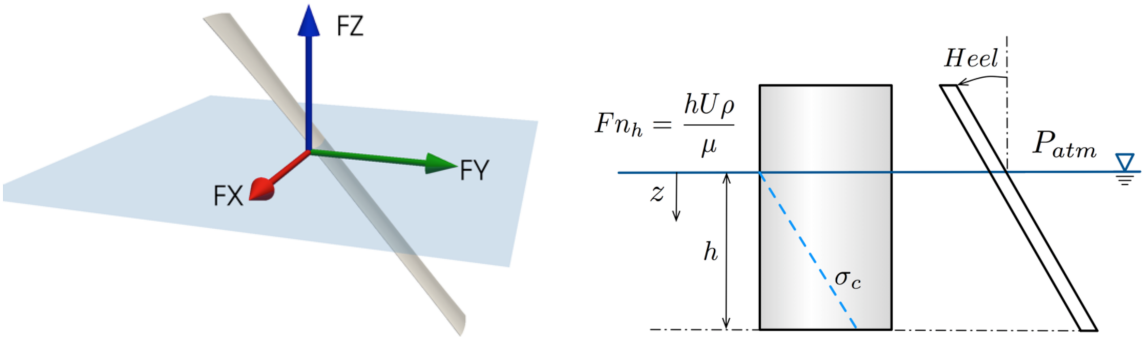

Figure 1: 3D model and 2D depiction of the condition to test.

Hereafter the resume Table 1 with testing conditions and non-dimensional parameters for ventilation probability check in upwind conditions.

Table 1: Testing conditions.

U	Heel	Yaw	Rake	h	Fn_h	Cl limit
20 kts	0°	0° to 3°	0° to 5°	4.24	0.6m	0.28
20 kts	60°	0° to 3°	0° to 5°	6.0	0.3m	0.14

In the conditions indicated in the previous table, ventilation could be present because of the large Fn_h and yaw angle greater than the bifurcation angle.

2.1 Low-fidelity methods

The initial phase for the design of a surface-piercing strut is the definition of the 2D section under the prescribed working conditions. Preliminary 3D planform design is tested by using a Vortex-Lattice Method (VLM). In case of 2D sections, the effect of the free surface is not taken into account; for the 3D VLM planform design/test, the presence of the free surface is taken into account imposing the anti-mirror boundary conditions at z=0.

As described before, a good indicator for ventilation probability is σ_v, which could be estimated also in 2D by using the Cp distribution of the hydrofoil section. Negative values of Cp at nose indicate tendency to ventilate or cavitate. Two candidate sections for kite foil mast strut are tested in 2D panel code tool in the expected Reynolds number and Angle of Attack (AoA = 3°).

Section 2 shows a lower min Cp distribution from the nose up to the first 40% of the profile, Figure 2. Gradient of Cp gives indication about how the profile is tolerant and it is correlated to the local curvature. It is interesting to see how the gradient of ventilation probability, in this case gradient of Cp, is correlated to the local section curvature. The 2D section with monotonic and smooth curvature (Section2) has lower leading edge ventilation probability respect compared to the 2D section with

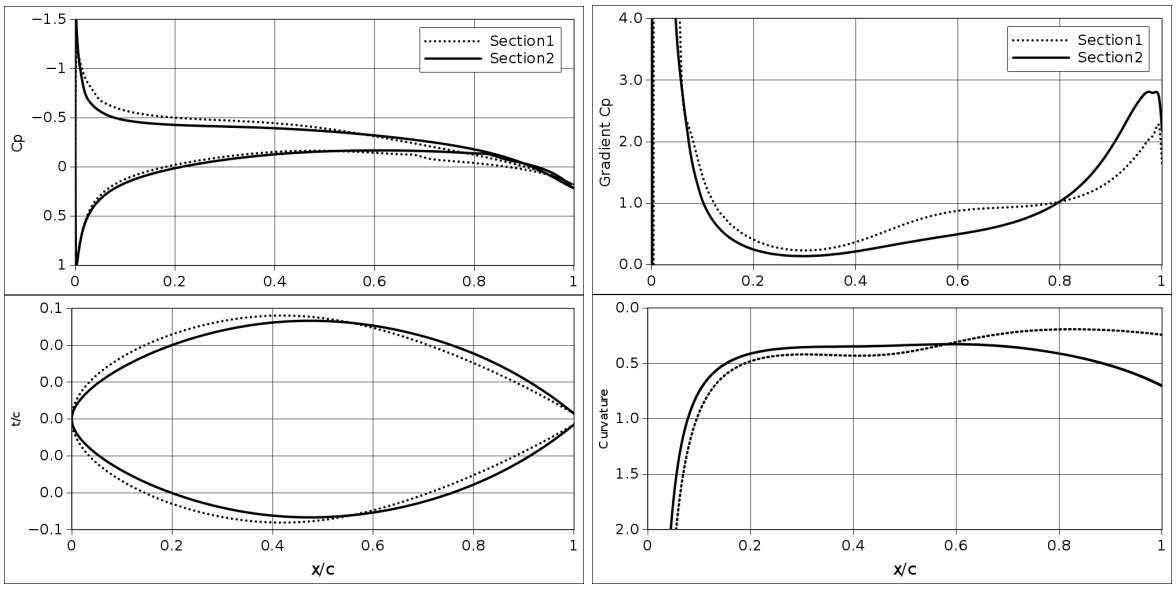

(a) Cp distribution **(b)** Gradient of Cp and curvature

Figure 2: Cp, Gradient of Cp and curvature.

varying and non-monotonic curvature (Section1). The gradient pressure direction change for the Section2 at the trailing edge indicates possible tail ventilation. These indications are useful for the 3D preliminary design via VLM methodology. The target of the 3D low-fidelity investigation is to depict the cases where the estimated lift is near the limit for stable ventilation.

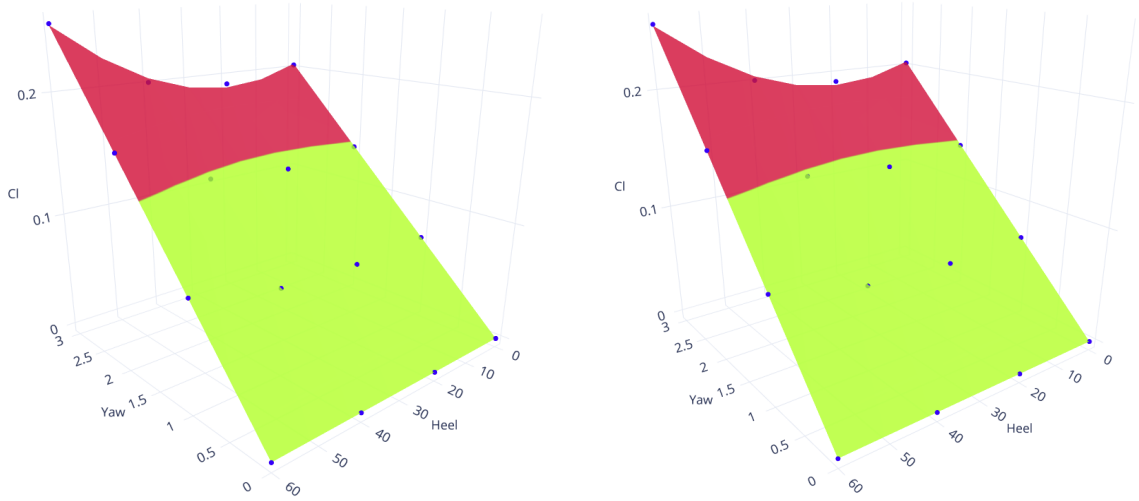

(a) Section1 **(b)** Section2

Figure 3: VLM Cl response surfaces.

Figure 3 shows the response surface of the VLM model with highlighted in red the conditions where the estimated Cl is exceeding the limits for possible ventilation. The choosen limit is the lower one to be in the safety zone. As reported from 2D section tests, Section2 shows a lower lift in the same running attitude, with less differences respect the 2D, which means again less probability of ventilation. The small difference between the two sections is not enough to define a strong trade-off in term of design advices; because of the nature of the methods used, it is not possible to take into account the presence of the disturbed free surface and have a good estimation of the ventilation probability. For this complex phenomenon, high-fidelity (Navier-Stokes solver) simulations are necessary; the 3D surface piercing strut is simulated in cases selected by preliminary results done via VLM code, cases

where the generated lift presents values exceeding the ventilation limits (high heel angle with yaw and rake condition).

For the mesh/solver strategy, the results from the CFD verification procedure are used for the definition of the mathematical representation of the surface-piercing strut. Cases with higher lift are the extreme ones, typical upwind conditions during a kite foil regatta; these cases are the most suitable for ventilation. Before testing the different struts it is necessary to verify the methodology and define the simulation uncertainties for a successive validation.

2.2 High-fidelity methods

2.2.1 Methodology for verification procedure

Having the results of three CFD simulations with different refinement sizes (meshes or time step - G0, G1, G2, with G0 finer mesh), it is possible to verify the accuracy of the mathematical model by using the classical Verification & Validation process. This method was proposed by Roache 1994, with the estimation of the Grid Convergence Index (GCI) able to estimate the spatial and temporal discretization uncertainties. The ratio of convergence is defined as:

$$R_k = \frac{\epsilon_{k_{21}}}{\epsilon_{k_{32}}}, \tag{4}$$

where $\epsilon_{k_{21}}$=G0-G1 is the difference between the solution values of the fine-medium grid and $\epsilon_{k_{32}}$=G1-G2 is the difference between the solution values of medium-coarse grid. To achieve a monotonic convergence, the value of needs to be in the range $0 < R_k < 1$. For the monotonic convergence, Richardson Extrapolation (RE) is used to estimate the uncertainty of the error of the generic grid and a theoretical grid with an infinite degree of refinement. In GCI approach, the uncertainty U_k is defined by using the error estimated with the generalized RE multiplied by a safety factor Fs:

$$U_k = Fs|\delta_{RE_{k1}}|, \tag{5}$$

where $\delta_{RE_{k1}}$ is the error estimated with the finer mesh.

2.2.2 Experimental benchmark

Considering the ventilation problem affecting kite foil masts, a proper benchmark for CFD is evaluated and simulation uncertainties are computed. The reference geometry is a surface-piercing strut tested in calm water at different AoAs and speeds. Experimental setup and data is described in Harwood *et al.* 2016. The test condition taken into account for the numerical comparison is at $Fn_h = 2.5$, submerged aspect ratio $(AR_h) = 1$ and angle of attach is AoA 25°; reference chord (c) is 0.279m. This corresponds to the following dimensional parameters: $U = 4.13$ m/s, depth (h) = 0.2794 m.

In the CFD simulations, the leading edge (LE) of the foil is fixed at x = 0 and the flow is from positive x. Velocity inlet boundary conditions are used in the whole domain except for the outflow patch where a proper zero-gradient boundary condition is applied; control volume extents in the x, y, and z directions respectively $9c$ aft strut trailing edge, $2c$ fwd strut leading edge, $5c$ on both sides and $4c$ top-bottom respect the initial free surface, again with c the chord length.

Initial mesh used for the CFD benchmark has 6.5M elements; a finer mesh (15M) and a coarser mesh (2.5M) are tested for spatial discretization uncertainty estimation. Solver non-dimensional time step for the simulation is based on mean convective Courant number around 0.1: $\Delta T \cdot U/c = 0.002$, where U is the steady target. Two coarser time steps ($\Delta T \cdot U/c = 0.004$ and $\Delta T \cdot U/c = 0.008$) are evaluated for verification purpose. Results from the verification procedure are reported in the following tables:

Table 2: Drag verification.

	r_{21}	R_k	p	ϵ_{32}	ϵ_{21}	U_{k32}	U_{k21}	U_{k_c}
Time	1.2599	0.67	1.754	0.12%	0.084%	0.31%	0.21%	0.042%
Mesh	1.3447	0.45	1.885	2.26%	1.03%	3.02%	1.72%	0.34%

Table 3: Lift verification.

	r_{21}	R_k	p	ϵ_{32}	ϵ_{21}	U_{k32}	U_{k21}	U_{k_c}
Time	1.2599	0.72	1.408	0.042%	0.031%	0.138%	0.099%	0.019%
Mesh	1.3447	0.41	2.184	2.014%	0.829%	2.176%	1.139%	0.228%

Considering the initial mesh (6.5M) and initial time step, uncertainty for Lift estimation is 2.276% and for Drag estimation is 3.23%. Mesh refinement has more impact on the uncertainty estimation respect the time step; this is mainly related to the initial time step which permits the solver to not exceed the limit of Courant = 1 for the coarse time step with the medium mesh. Numerical free surface shows a good correlation with the experimental visualization. Data comparison extracted from experimental data and from CFD is reported on the following table:

Table 4: EFD vs CFD.

	Cd	Cl	$error - Cd$	$error - Cl$
EFD	0.231	0.423	-	-
CFD	0.239	0.429	3.6%	1.2%

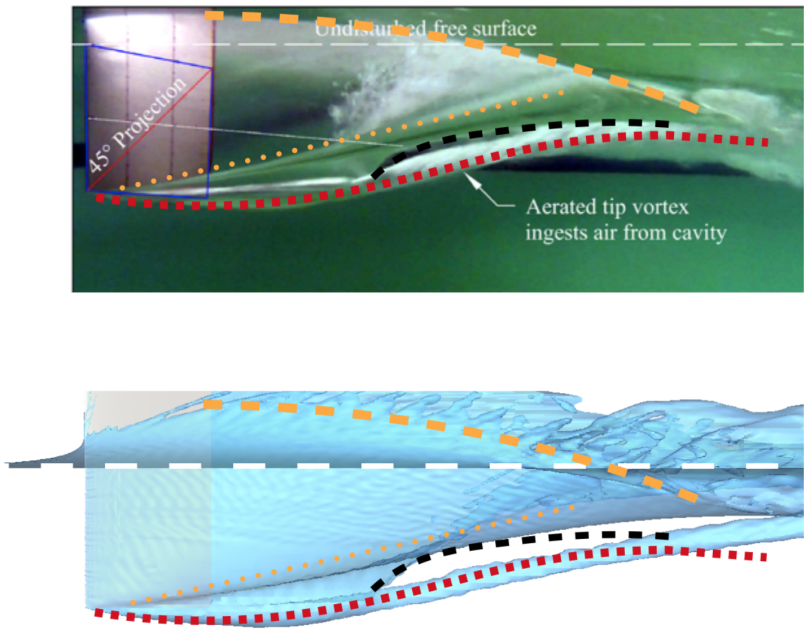

Figure 4: EFD vs CFD freesurface comparison.

2.2.3 Application

For each section, the higher lift condition achieved with VLM method was simulated with RANS approach, using the same methodology verified by using the experimental benchmark. Because with RANS approach it is possible to consider the effect of free surface, ventilation probability distribution is mapped on the 3D surface and gives indication about the possibility of leading edge or tail ventilation.

Comparing the 3D mapped solution, Figure 5, it is evident that the Section2 is less tolerant to tail ventilation; the distribution of ventilation inception probability shows a connection of negative zones with the trailing edge of the struct, which means opening a way to inflate air from the free surface. For leading edge ventilation, σ_v distribution shows a similar pattern with Section1 with small gradient in span-wise direction, Figure 6; in this case near the free surface chord-wise direction there is a persistent low-pressure region, which help air to enter from above the free surface and produce a ventilated cavity.

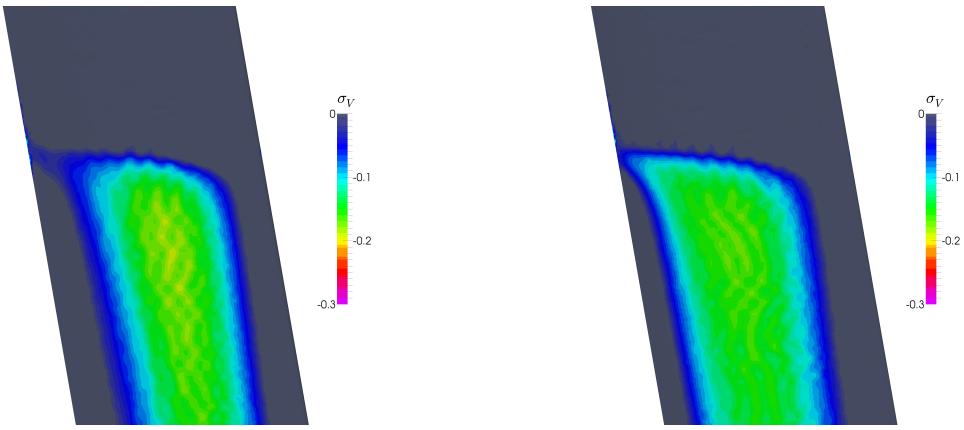

(a) Section1 **(b)** Section2

Figure 5: σ_v distribution; flow is going right to left.

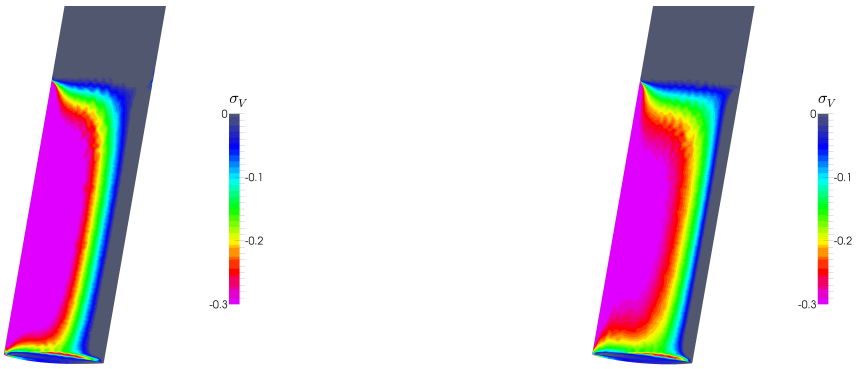

(a) Section1 **(b)** Section2

Figure 6: σ_v distribution; flow is going left to right.

Because section curvature and pressure are strictly correlated, statistical approach could be used to analyze the possibility of leading edge ventilation. Considering the normalized distribution of curvature and σ_v, a 3D mapping of the Mahalanobis distance (Mahalanobis 1936) highlights the differences between the two sections. The Mahalanobis distance is a measure between a sample point and a distribution. The Mahalanobis distance from a vector $\mathbf{y}$ to a distribution with mean μ and covariance $\sum$ is defined as:

$$d^2 = (\mathbf{y} - \mu) \sum^{-1} (\mathbf{y} - \mu), \tag{6}$$

This distance represents how far y is from the mean in number of standard deviations. The more the distance, the more the curvature affects the pressure distribution and the probability of ventilation inception. As shown in the Figure 7, Section1 is more prone to ventilate by leading edge.

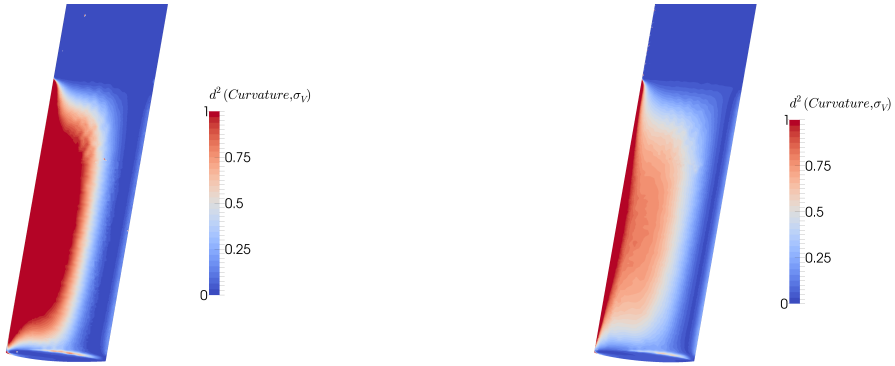

(a) Section1 **(b)** Section2

Figure 7: Mahalanobis distance.

3 CONCLUSIONS

Kite foil masts are acting as surface piercing struts and could be affected by ventilation. The design of a kite foil mast must be done considering the interaction with disturbed free surface. Initial indication could be extracted from 2D simulations but high-fidelity ones are necessary to understand the probability of ventilation. Both leading edge and trailing edge ventilations are strictly related to local pressure and free surface deformation. Here main finding of the investigation:

- 2D and 3D low-fidelity methods are effective for initial design but high-fidelity models are necessary to understand the complexity of ventilation;
- Tail ventilation is easier to detect by using σ_v distribution;
- Leading edge ventilation is more difficult to predict and a possible method to visualize the tendency of that is to use a statistical way which correlate the local surface curvature with local σ_v distribution;

Further investigations and validations are necessary to confirm the information extracted from this analysis.

REFERENCES

Barden T., Binns J. (2012). On the Road to Establishing Ventilation Probability for Moth Sailing Dinghies. 18th Australasian Fluid Mechanics Conference. 3-7 December, Launceston, Tasmania, Australia

Binns J., Ashworth B. A., Fleming A., Duffy M., Haase J., Kermarec M. (2017). Unlocking hydrofoil hydrodynamics with experimental results. Proceedings of the 4th International Conference on Innovation in High Performance Sailing Yachts, 29-30 June, Lorient, France.

Breslin J. P., Skalak R. (1959). Eploratory Study of Ventilated Flows about Yawed Surface-Piercing Struts). NASA Technical Memorandum, Washington, DC, Technical Report No. 2-23-59W.

Fridsma G. (1963). Ventilation Inception on a Surface Piercing Dihedral Hydrofoil With Plane Surface Wedge Section. Davidson Laboratory, Stevens Institute of Technology, Hoboken, NJ, Technical Report No. 952.

Harwood, C. M., Young, Y. L., Ceccio S. L. (2016). Ventilated cavities on a surface-piercing hydrofoil at moderate Froude numbers: Cavity formation, elimination and stabilit. J. Fluid Mech., vol. 800, no. August, pp. 5-56.

Young Y. L., Harwood C. M., Miguel M. F., Ward J.C., Ceccio S. L. (2017).Ventilation of Lifting Bodies: Review of the Physics and Discussion of Scaling Effects. Appl. Mech. Rev., vol. 69, no. 1, p. 010801.

Young Y. L., Brizzolara S. (2013). Numerical and Physical Investigation of a Surface-Piercing Hydrofoil. Third International Symposium on Marine Propulsors smp13, Launceston, Tasmania, Australia, May 2013, pp. 1-8.

Mahalanobis, P. C. (1936). On the generalised distance in statistics. Proceedings of the National Institute of Sciences of India, vol. 2, n.1, pp. 49-55.

Roache, P. (1994). Perspective: a method for uniform reporting of grid refinement studies. ASME J. Fluids Eng. 116, pp. 405-413

Swales P. D., Wright A. J., McGregor R. C., Rothblum R. (1974). The Mechanism of Ventilation Inception on Surface Piercing Foils. J. Mech. Eng. Sci., vol. 16, no. 1, pp. 18-24.

Taylor G.T. (1950) The instability of liquid surfaces when accelerated in a direction perpendicular to their planes. Proc. R. Soc. London. Ser. A. Math. Phys. Sci., vol. 201, no. 1065, p. 192 LP-196.